Inflammation, Vol. 42, No. 4, August 2019 (© 2019)
DOI: 10.1007/s10753-019-01011-3

ORIGINAL ARTICLE

Probucol Ameliorates Complete Freund's Adjuvant-Induced Hyperalgesia by Targeting Peripheral and Spinal Cord Inflammation

Amanda Z. Zucoloto,[1,2,3] Marília F. Manchope,[1] Sergio M. Borghi,[1] Telma S. dos Santos,[1] Victor Fattori,[1] Stephanie Badaro-Garcia,[1] Doumit Camilios-Neto,[4] Rubia Casagrande,[5] and Waldiceu A. VerriJr[1,6]

Abstract— The effect of the lipid-lowering agent probucol in inflammatory hyperalgesia and leukocyte recruitment was evaluated in a model of subacute inflammation by Complete Freund's adjuvant (CFA). As CFA induces long-lasting nociception characterized by peripheral and spinal cord inflammation, the anti-inflammatory activity of probucol was assessed at both foci. Probucol at 0.3–3 mg/kg was administrated per oral daily starting 24 h after CFA intraplantar injection. Mechanical and thermal hyperalgesia induced by CFA were determined using an electronic anesthesiometer and hot plate apparatus, respectively. Post-treatment with probucol at 3 mg/kg inhibited CFA-induced hyperalgesia over the course of 7 days as well as paw edema. Overt pain-like behaviors, which were determined by the number of flinches and time spent licking paw immediately following CFA injection, were also reduced by probucol at 3 mg/kg administered as a pre-treatment. To investigate the mechanisms underlying the analgesic effect of probucol, neutrophil recruitment to paw was assessed by myeloperoxidase activity, cytokine production, *Cox-2* expression, and NF-κB activation in both paw and spinal cord by ELISA. Iba-1, GFAP, and substance P protein expression and nuclear localization of phosphorylated NF-κB were evaluated in the spinal cord by immunofluorescence. Probucol at 3 mg/kg attenuated neutrophil recruitment, cytokine levels, and NF-κB activation as well microglia and astrocyte activation, and substance P staining in the spinal cord. Taken together, the results suggest that probucol exerts its analgesic and anti-inflammatory activity in an

[1] Departamento de Ciências Patológicas, Centro de Ciências Biológicas, Universidade Estadual de Londrina, Londrina, Brazil
[2] Snyder Institute for Chronic Diseases, University of Calgary, HRIC 4C51, 3230 Hospital Dr NW, Calgary, AB T2N 4N1, Canada
[3] Department of Microbiology, Immunology, and Infectious Diseases, University of Calgary, HRIC 4C51, 3230 Hospital Dr NW, Calgary, AB T2N 4N1, Canada
[4] Departamento de Bioquímica e Biotecnologia, Centro de Ciências Exatas, Universidade Estadual de Londrina, Londrina, Brazil
[5] Departamento de Ciências Farmacêuticas, Centro de Ciências da Saúde, Universidade Estadual de Londrina, Londrina, Brazil
[6] To whom correspondence should be addressed at Departamento de Ciências Patológicas, Centro de Ciências Biológicas, Universidade Estadual de Londrina, Londrina, Brazil. E-mail: waldiceujr@yahoo.com.br

experimental model of persistent inflammation by targeting the NF-κB pathway in peripheral and spinal cord foci.

KEY WORDS: subacute inflammation; probucol; pain; nociception; CFA.

INTRODUCTION

Pain is a cardinal feature of inflammation and an evolutionary mechanism of self-preservation. Nonetheless, persistence of noxious stimuli and impairment in resolution processes underlie the pathogenesis of most chronic inflammatory diseases [1, 2]. Pathological pain is a comorbidity of many chronic diseases and an emerging public health concern with social and economic implications. Therefore, treating chronic pain is of great importance as it affects patient's quality of life and productivity [3–5]. The side effects associated with long-term use of steroidal or non-steroidal anti-inflammatory drugs challenge the treatment of chronic diseases [6, 7]. In that sense, developing alternative therapies is of great relevance worldwide. Experimental models of subacute inflammation and persistent pain have been useful to screen and characterize the analgesic and anti-inflammatory potential of novel compounds or repurposing drugs already available in the market.

Complete Freund adjuvant (CFA) is made of non-metabolizable oils and heat killed *Mycobacterium tuberculosis* (MTB). MTB cell wall structures are sensed by at least toll-like receptors (TLRs) 1, 2, and 4, among other PRRs, such as NOD2 and Dectin-1 [8–11]. MTB cell wall glycolipids and lipoproteins activate TLR2 leading to TNF-α and IL-1β production in macrophages [12, 13]. Signaling through Dectin-1 and NOD2 also induces production of pro- and anti-inflammatory cytokines, *e.g.*, TNF-α, IL-6, and IL-10 [10, 11]. Means et al. (2001) demonstrated the crucial role of TLR2 and TLR4 in triggering the NF-κB pathway in macrophages stimulated with MTB [9].

CFA induces long-lasting nociception characterized by glial activation, substance P mobilization, and spinal cord production of pro-inflammatory mediators as early as 4 h culminating in thermal and mechanical hyperalgesia for up to 14 days post-injection [14, 15]. Inflammatory mediators increase upon CFA administration such as the pro-inflammatory cytokines (IL-1β, TNF-α, and IL-6) in both peripheral tissues as well as the spinal cord [15]. Therefore, the CFA model is a well-established model for evaluating the analgesic mechanisms of novel compounds in all stages of the inflammatory response, *i.e.*, acute, subacute and chronic.

Probucol is a synthetic polyphenolic compound first exploited as a lipid-lowering agent [16]. However, the beneficial effects of probucol were shown to go beyond the lipid metabolism as its antioxidant and anti-inflammatory mechanisms started to be unveiled. For instance, probucol acts as a superoxide anion scavenger *in vitro* [17]. It was also shown to inhibit the production of pro-inflammatory and pro-hyperalgesic mediators as well as expression of adhesion molecules and NF-κB activation *in vitro* [18–23]. These mechanisms likely contribute to the beneficial effects of probucol observed in experimental models of atherosclerosis, neurodegenerative diseases, and diabetes [24–27]. Furthermore, we have previously demonstrated the analgesic and anti-inflammatory effect of probucol in models of acute inflammation [28, 29]. These studies, however, investigated the effect of probucol as a pre-treatment, in a short-term period (no longer than 6 h post-stimulus) and only peripheral mechanisms were evaluated.

Given these previous studies, we sought to evaluate the analgesic potential of probucol in the CFA model of persistent pain, in a post-treatment regimen. To further investigate the mechanisms involved in its antinociceptive mechanisms, we evaluated the production of pro-inflammatory and pro-hyperalgesic mediators as well as NF-κB activation in peripheral tissue and in the spinal cord. We have also evaluated the effect of probucol on glial cell activation in the spinal cord as a readout of inflammation.

MATERIALS AND METHODS

Animals

Male Swiss mice (20–25 g) from Universidade Estadual de Londrina, Parana, Brazil, were used in this study. Mice were housed in standard clear plastic cages, and received food and water *ad libitum* under a 12:12 h light/dark cycle at 21 °C. All behavior tests were performed between 9 a.m. and 5 p.m. in temperature-controlled room. The Animal Welfare and Ethics Committee of Londrina State University approved this study

(process number 1012.2015.74). All efforts were made to minimize the number of animals used and their suffering.

Drugs

Materials were obtained from the following sources: Complete Freund Adjuvant (Sigma-Aldrich, St. Louis, MO, USA), Diclofenac (Neoquímica, Anápolis, GO, Brazil), Indomethacin (Sigma-Aldrich, St. Louis, MO, USA), Acetaminophen (Santa Cruz Biotechnology, Dallas, TX, USA), and Probucol (Santa Cruz Biotechnology, Dallas, TX, USA).

Experimental Procedures

Mice were treated with probucol (0.3, 1, 3 mg/kg, per oral) or vehicle (Tween 80 5% in saline) daily 24 h after the administration of CFA (10 μL/paw). Mechanical hyperalgesia, thermal hyperalgesia, and paw edema were evaluated 3 h after treatment for 7 days. Paw skin was removed to assess neutrophil recruitment by myeloperoxidase (MPO) activity assay 7 days after CFA injection. Protein expression of Iba-1, GFAP, and substance P were evaluated 3 days after CFA i.pl. injection. Antioxidant effect (effect on the ability to scavenge the ABTS radical, superoxide anion production [NBT assay], and lipid peroxidation [TBARS assay]), cytokine production (TNF-α, IL-6, IL-1β, and IL-10), and NF-κB activation (p-NF-κB p65/total NF-κB p65 ratio and nuclear localization of p-NF-κB p65) were evaluated in paw and spinal cord (L4-L6) 3 days after CFA i.pl. *Cox-2* expression was evaluated in paw and spinal cord (L4-L6) 3 and 1 day after CFA i.pl. injection, respectively. Overt pain-like behavior was induced by CFA (10 μL/paw), and the number of flinches and time spent licking the paw were evaluated during 30 min right after CFA injection. In these set of experiments, particularly mice were treated with probucol 1 h before CFA stimulus. Doses of stimulus and time points of sample collection were based on previous studies [15, 30, 31].

Mechanical Hyperalgesia Test

Mechanical hyperalgesia was assessed by an electronic version of von Frey filaments [32]. A handheld force transducer (electronic anesthesiometer; Insight, Ribeirao Preto, SP, Brazil) adapted with a 0.5-mm^2 polypropylene tip was used to evoke hind paw nociceptive withdrawal response. The intensity of the pressure (in g) at the moment of paw withdrawal was automatically recorded. The mechanical threshold was tested before (baseline) and after CFA i.pl. administration (10 μL/paw). The results are expressed as delta (Δ) withdrawal threshold (in g), obtained by subtracting the measurements at each time point (1 to 7 days after i.pl. CFA injection) from the baseline values.

Thermal Hyperalgesia Test

Animals were placed on a hot plate apparatus (Insight, Ribeirao Preto, SP, Brazil) at a constant temperature of 52 °C. The end-point was characterized by removal of the paw followed by flinching or licking the paw, and latency time until the end-point reaction was determined [33]. Maximum latency until end-point was set at 20 s to avoid tissue damage. The results are expressed as means of latency (s) within experimental groups.

Myeloperoxidase Assay

Myeloperoxidase (MPO) colorimetric assay was performed as an indirect indicator of neutrophil recruitment to paw tissue. Paw skin samples were collected 7 days after CFA injection and homogenized in ice-cold K_2HPO_4 buffer (400 μL, 50 mM, pH 6.0) containing HTAB (0.5% weight/volume) using a tissue-tearor (Biospec, Bartlesville, OK, USA). Samples were centrifuged (16,100*g* × 2 min × 4 °C), and the supernatants were used. The MPO activity assay was performed as previously described [34]. Briefly, 50 mM phosphate buffer, pH 6.0 containing 0.167 mg/mL o-dianisidine dihydrochloride, and 0.015% hydrogen were added to samples, and the absorbance was read at 450 nm (Multiskan GO Microplate Spectrophotometer, Thermo Scientific, Vantaa, Finland). The values obtained were compared to a standard curve of neutrophils, and results are expressed as MPO activity (neutrophils × 10^6/g of tissue).

Paw Edema

Paw edema was measured using a dial thickness gauge 0–20 mm (Mitutoyo, Andover, Hampshire, UK). The results are expressed as paw thickness (in mm). The values were obtained by subtracting the baseline values from the measurements obtained at each time point (1 to 7 days after i.pl. CFA injection).

Spinal Cord Immunofluorescence

Spinal cord samples were collected 3 days after stimulus (CFA 10 μL/paw). Mice were perfused through the ascending aorta with saline followed by 4% paraformaldehyde. The spinal cord (L4-L6) was then dissected out, post-fixed, and replaced overnight

in 30% sucrose. To obtain tissue sections, the spinal cord segments were embedded in optimum cutting temperature (O.C.T.) using Tissue-Tek® (Sakura® Finetek, Torrance, CA, USA). Ten-micromolar sections were obtained in a cryostat (CM1520, Leica Biosystem, Richmond, IL, USA). For immunofluorescence processing, sections were blocked with buffer solution (500 μL per slide, PBS, 0.1% Tween 20, 5% BSA) for 2 h and further incubated with primary antibodies against GFAP (180,063; Invitrogen, Life Technologies, Carlsbad, CA, USA), Iba-1 (PA5–27436; Invitrogen, Life Technologies, Carlsbad, CA, USA), phosphorylated NF-κB p65 subunit (sc-136,548; Santa Cruz Biotechnology, Dallas, TX, USA), or substance P (sc-21,715; Santa Cruz Biotechnology, Dallas, TX, USA) overnight at −4 °C. 4′,6-Diamidino-2-phenylindole (DAPI) was used for nuclear staining. The following day, slides were washed and incubated with secondary antibodies conjugated with Alexa Fluor 488 (#A-110088; Thermo Fisher Scientific, Waltham, MA, USA) or Alexa Fluor 647 (#4418S; Cell signaling, Danvers, Massachusetts, USA) for 1.5 h at room temperature. Image capturing and quantitative analysis were performed in a confocal microscope (TCS SP8, Leica Microsystems, Mannheim, Germany) [35, 36]. For quantification of immunostaining, equivalent areas of the spinal cord across the groups were selected, and results were expressed as fluorescence intensity. Pearson's correlation coefficient was used as a measure of the nuclear localization of p-NF-κB p65 subunit, as observed by the colocalization between areas positive for DAPI staining and p-NF-κB p65 subunit.

Total Antioxidant Capacity

Antioxidant capacity was assessed by the ABTS assay. This test was adapted to a 96-well microplate format as previously described [31]. Paw skin and spinal cord (L4-L6) samples were collected 3 days after stimulus (CFA 10 μL/paw) and homogenized with a tissue-tearor in ice-cold KCl buffer (500 μL, 1.15% *w*/*v*). Samples were centrifuged at 835 *g* at 4 °C for 10 min, and supernatants were used. ABTS assay was performed as an indicator of the sample's ability to scavenge the free radical ABTS. Diluted ABTS solution was added to samples, and the absorbance was measured at 730 nm after 6 min of incubation at 25 °C (Multiskan GO, Thermo Scientific). The results were equated against a standard Trolox curve (0.02–20 nmol) and expressed as nanomole Trolox eq. per milligram of tissue.

Superoxide Anion Production

Superoxide anion production was assessed by the NBT assay. Paw skin and spinal cord (L4-L6) samples were collected 3 days after stimulus (CFA 10 μL/paw). Samples were homogenized with a tissue-tearor in 500 μL of ice-cold KCl buffer (1.15% *w*/*v*), and the homogenates were used for the assay. The test was adapted to a microplate as previously described [37]. The NBT reduction was measured at 600 nm (Multiskan GO, Thermo Scientific). The results are expressed as optical density (OD) per milligram of tissue.

Lipid Peroxidation

Lipid peroxidation was measured by the TBARS (Thiobarbituric Acid Reactive Substances) assay. Paw skin and spinal cord (L4-L6) samples were collected 3 days after stimulus (CFA 10 μL/paw) and homogenized with a tissue-tearor in ice-cold KCl buffer (500 μL, 1.15% *w*/*v*). The test was adapted to a microplate as previously described [37]. The intermediate product of lipid peroxidation malondialdehyde (MDA) was determined by subtracting the absorbance at 535 nm from the absorbance at 572 nm (Multiskan GO, Thermo Scientific). The results are expressed as nanomoles of MDA per milligram of tissue.

Cytokine Measurement

Paw skin and spinal cord (L4-L6) samples were collected 3 days after stimulus (CFA 10 μL/paw). Samples were homogenized with a tissue-tearor in 500 μL of ice-cold buffer with protease inhibitors followed by centrifugation (835 *g* × 15 min × 4 °C). The supernatants of paw skin and spinal cord homogenates were used to determine TNF-α, IL-6, IL-1β, and IL-10 levels by enzyme-linked immunosorbent assay (ELISA) using commercial kits (eBioscience, San Diego, CA, USA). Absorbance was measured at 450 nm (Multiskan GO, Thermo Scientific). The results are expressed as picograms of cytokines per 100 mg of tissue.

Reverse-Transcriptase and Quantitative PCR

Paw and spinal cord tissue samples were collected 1 or 3 days after stimulus, respectively (CFA 10 μL/paw). Samples were homogenized in TRIzol® reagent (Life Technologies), and total mRNA was isolated according to manufacturer's directions. RNA purity was confirmed by the 260/280 ratio. Reverse-Transcriptase PCR (RT-PCR) was performed as previously described [33]. Quantitative PCR (qPCR) was performed using GoTaq® 2-Step

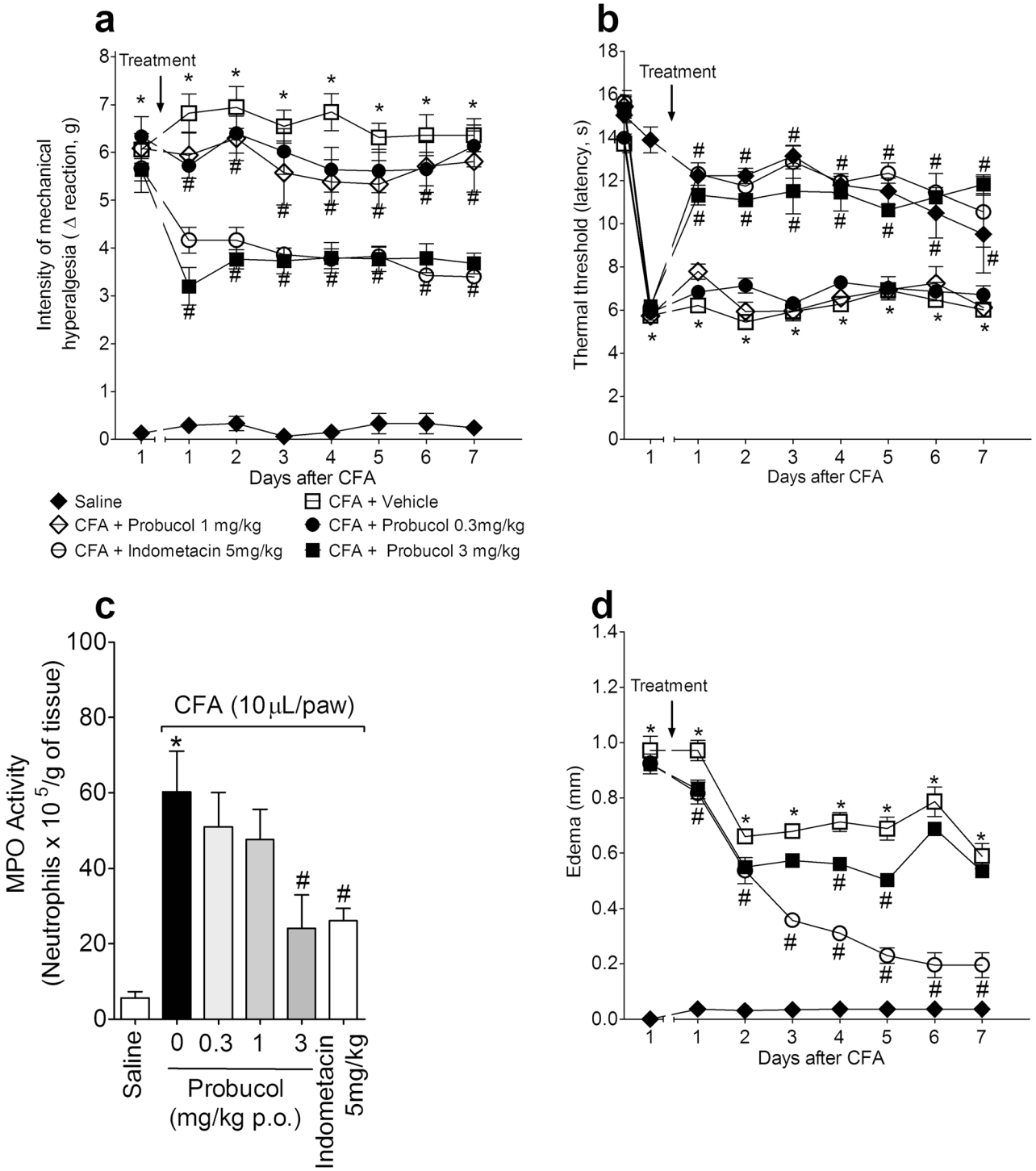

Fig. 1. Probucol inhibits CFA-induced mechanical and thermal hyperalgesia, neutrophil recruitment, and paw edema. Mice received probucol at doses 0.3, 1, and 3 mg/kg (p.o.) daily 24 h after i.pl. injection of CFA (10 μL/paw). Mechanical (**a**) and thermal (**b**) hyperalgesia and paw edema (**d**) were evaluated 3 h after treatment for 7 days. MPO (**c**) activity was assessed 7 days after CFA stimulus. Results are expressed as mean ± SEM ($n = 6$ per group per experiment, representative of two separate experiments). Two-way repeated measures ANOVA or one-way ANOVA followed by Tukey's post hoc. *$p < 0.05$ *vs.* saline group. #$p < 0.05$ *vs.* vehicle group.

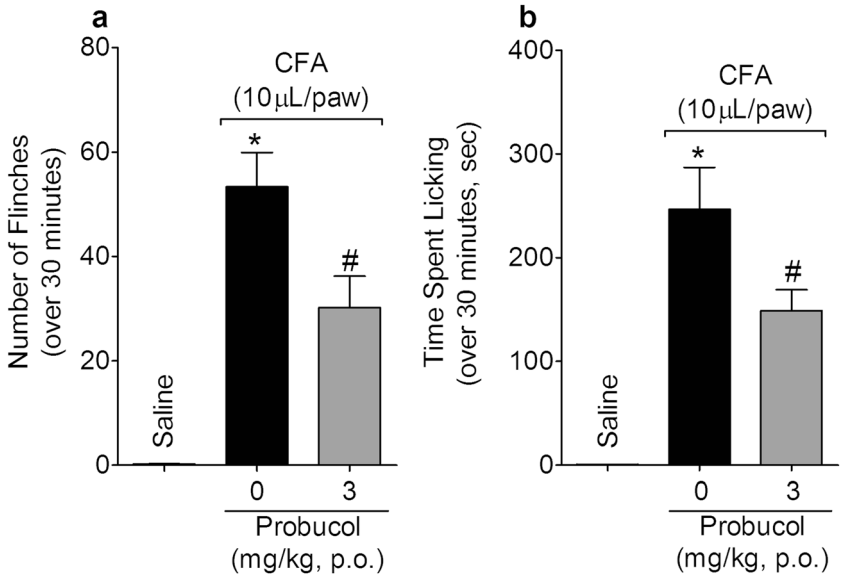

Fig. 2. Probucol inhibits CFA-induced overt pain-like behavior. Mice received probucol at 3 mg/kg (p.o.) 1 h before i.pl. injection of CFA (10 μL/paw). The number of flinches (**a**) and time spent licking the paw (**b**) were evaluated 0–30 min after i.pl. administration of CFA. Results are expressed as mean ± SEM ($n = 6$ per group per experiment, representative of two separate experiments). One-way ANOVA followed by Tukey's post hoc. *$p < 0.05$ *vs.* saline group. #$p < 0.05$ *vs.* vehicle group.

RTqPCR System (Promega) on a StepOnePlus™ Real-Time PCR System (Applied Biosystems®). The relative gene expression was measured using the comparative $2^{-(\Delta\Delta Cq)}$ method. The expression of *Gapdh* (glyceraldehyde 3-phosphate dehydrogenase) mRNA was used as a reference gene to normalize data. The primers used were the following: *Gapdh*, sense 5′CATACCAG GAAATGAGCTTG 3′, anti-sense 5′ ATGACATC AAGAAGGTGGTG 3′; and *Cox-2*, sense 5′ GTGGAAAAACCTCGTCCAGA 3′, anti-sense 5′ GCTCGGCTTCCAGTATTGAG 3′.

NF-κB Activation

Paw skin and spinal cord (L4-L6) samples were collected 3 days after stimulus (CFA 10 μL/paw). Samples were homogenized with a tissue-tearor in 400 μL of ice-cold lysis buffer (Cell Signaling, Danvers, MA, USA) followed by centrifugation (16,100 $g \times 10$ min × 4 °C). The supernatants were used for determination of phosphorylated NF-κB p65 subunit and total NF-κB p65 subunit levels using ELISA PathScan Kits (Cell Signaling, Danvers, MA, USA) according to the manufacturer's directions. Absorbance was measured at 450 nm (Multiskan GO, Thermo Scientific). The results are expressed as IOD ratio (p-NF-κB p65/total NF-κB p65).

Parameters of Drug Toxicity

To evaluate hepatotoxicity, plasma levels of aspartate aminotransferase (AST) and alanine aminotransferase (ALT) were measured using a diagnostic kit from Labtest (Lagoa Santa, Minas Gerais, Brazil) [38, 39]. Plasmatic AST and ALT levels in probucol-treated mice were compared to acetaminophen treatment (650 mg/kg, single dose), a hepatotoxic drug. The results are expressed as units per liter. In turn, nephrotoxicity was assessed by measurement of urea and creatinine in plasma also using a diagnostic kit from Labtest (Lagoa Santa, Minas Gerais, Brazil) [40]. The results are expressed as milligram per milliliter and were compared to diclofenac treatment (200 mg/kg, single dose). Gastric lesion was evaluated by performing the MPO kinetic-colorimetric assay as an indirect indicator of neutrophil recruitment in stomach [30]. The results are expressed as neutrophils per gram of tissue and were compared to indomethacin treatment.

Statistical Analyses

Results are presented as mean ± SEM of measurements made on four or six mice per group per experiment and are representative of two independent experiments. Two-way repeated measures analysis of variance (ANOVA) followed

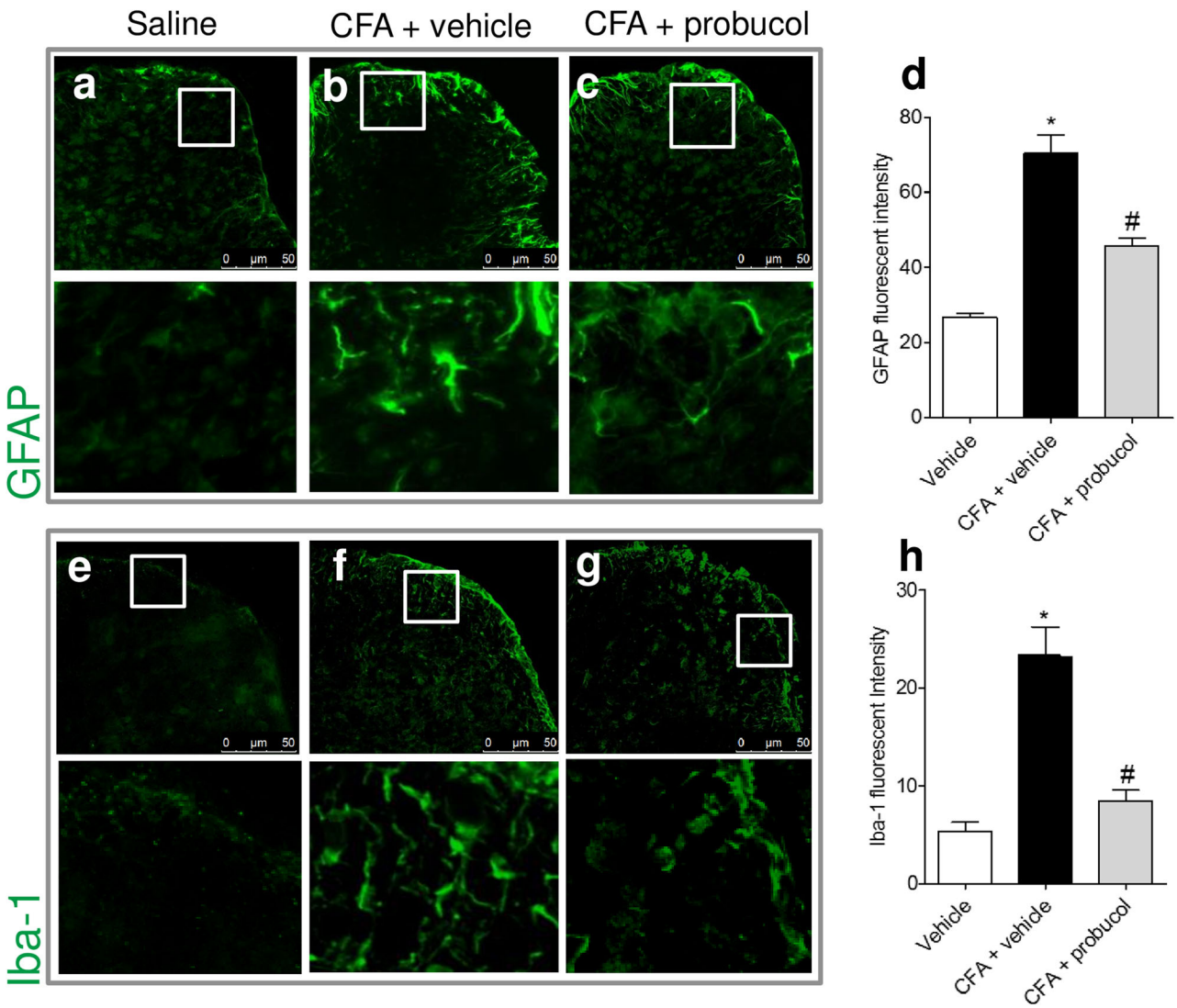

Fig. 3. Probucol inhibits CFA-induced glial activation in spinal cord. Mice received probucol at 3 mg/kg (p.o.) daily 24 h after i.pl. injection of CFA (10 µL/paw). Spinal cord tissue (L4–L6) was removed 3 days after CFA. GFAP and Iba-1 expression were evaluated by immunofluorescence. Representative images of GFAP and Iba-1 in the spinal cord of each experimental group is shown in panels a-c and e-g, respectively. Quantification of GFAP and Iba-1 fluorescent intensity are shown in panels d and h, respectively. The 0 mg/kg of probucol group stands for vehicle group. Results are expressed as mean ± SEM ($n = 4$ per group per experiment, representative of two separate experiments). One-way ANOVA followed by Tukey's post hoc. *$p < 0.05$ *vs.* saline group. #$p < 0.05$ *vs.* vehicle group.

by Tukey's *post hoc* was used to compare groups and doses at all time points when responses were measured at different time points after stimulus injection (mechanical and thermal hyperalgesia tests and edema assessment). One-way ANOVA followed by Tukey's post hoc was performed for data from single time point experiments. $P < 0.05$ was considered statistically significant. All data analyses were performed using GraphPad Prism® 5.0 (GraphPad Software, Inc., USA-500.288), as well as elaboration of figures.

RESULTS

Probucol Inhibits CFA-Induced Mechanical and Thermal Hyperalgesia, Neutrophil Recruitment, and Paw Edema

Mice were treated with probucol at doses of 0.3, 1, and 3 mg/kg p.o. or vehicle (Tween 80 5% in saline) daily 24 h after i.pl. administration of CFA

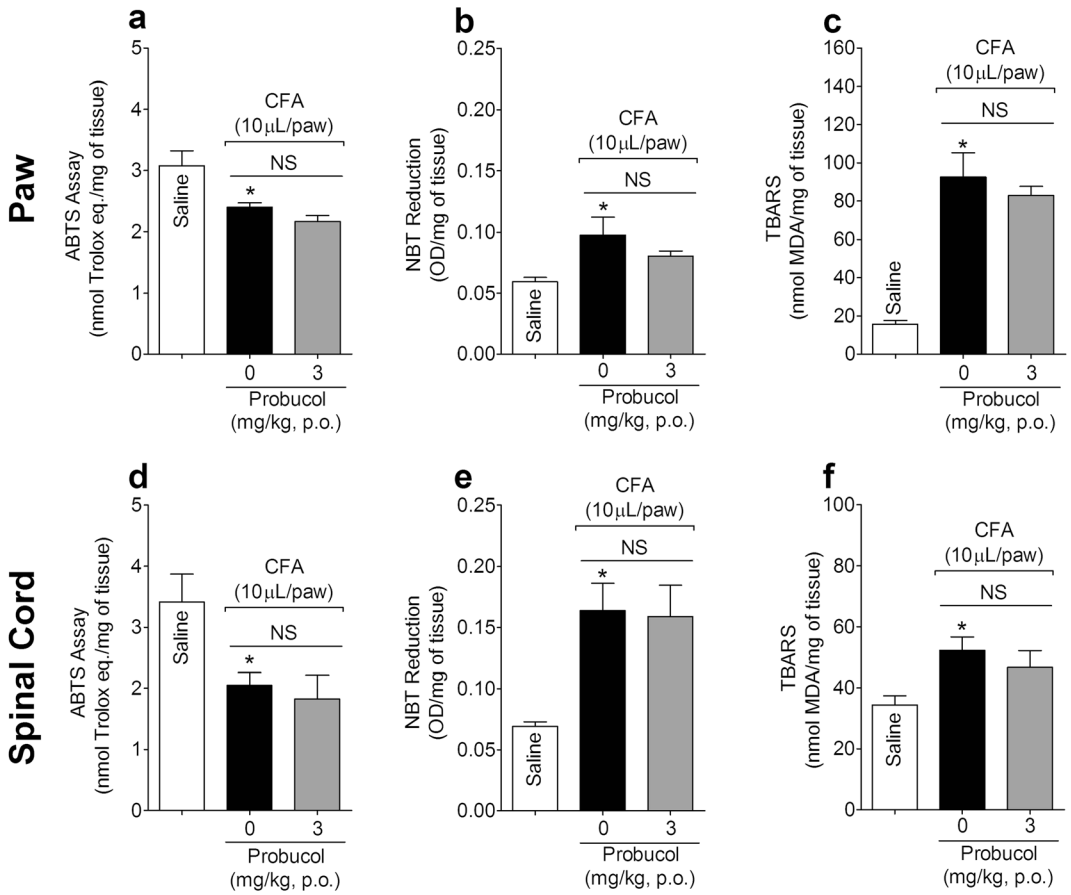

Fig. 4. Probucol does not inhibit CFA-induced ROS production in paw tissue and spinal cord. Mice received probucol at 3 mg/kg (p.o.) daily 24 h after i.pl. injection of CFA (10 μL/paw). Paw skin and spinal cord tissue (L4–L6) were removed 3 days after CFA. ABTS (**a**, **d**), NBT (**b**, **e**), and TBARS (**c**, **f**) assays were performed from paw skin and spinal cord. The 0 mg/kg of probucol group stands for vehicle group. Results are expressed as mean ± SEM ($n = 6$ per group per experiment, representative of two separate experiments). One-way ANOVA followed by Tukey's post hoc. *$p < 0.05$ *vs.* saline group. #$p < 0.05$ *vs.* vehicle group. NS stands for non-significant statistical differences.

(10 μL/paw). At day 1, mechanical and thermal hyperalgesia were evaluated 1, 3, 5, and 7 h after treatment. The analgesic effect was more prominent 3 h after treatment; thus, this time point was chosen to evaluate both mechanical and thermal hyperalgesia in the following days (data not shown). Probucol at 3 mg/kg reduced CFA-induced mechanical hyperalgesia at all time points, up to 45% (Fig. 1a). Thermal hyperalgesia was also reduced at all time points (up to 98%) (Fig. 1b). Probucol at the doses of 0.3 mg/kg or 1 mg/kg did not show analgesic effect ($p > 0.05$). Paw tissue was removed 7 days after CFA stimulus, and the samples were used to evaluate MPO activity, a marker of neutrophil recruitment. Probucol at 3 mg/kg reduced MPO activity in the paw skin (65%) similarly to the reference drug indomethacin, which showed a 62% MPO activity inhibition. In turn, the lower doses of probucol did not affect neutrophil recruitment ($p > 0.05$) (Fig. 1c). Therefore, the dose of 3 mg/kg was chosen for the next experiments. Paw edema was evaluated over the course of 7 days as well. A significant reduction of paw edema by probucol was only observed at days 1, 4, and 5 (up to 26%, at day 5). In turn, indomethacin inhibited edema at all time points ($p < 0.05$) (Fig. 1d).

Probucol Inhibits CFA-Induced Overt Pain-like Behavior

Mice were treated with probucol at 3 mg/kg (p.o.) 1 h before i.pl. injection of CFA (10 μL/paw). Overt pain-like

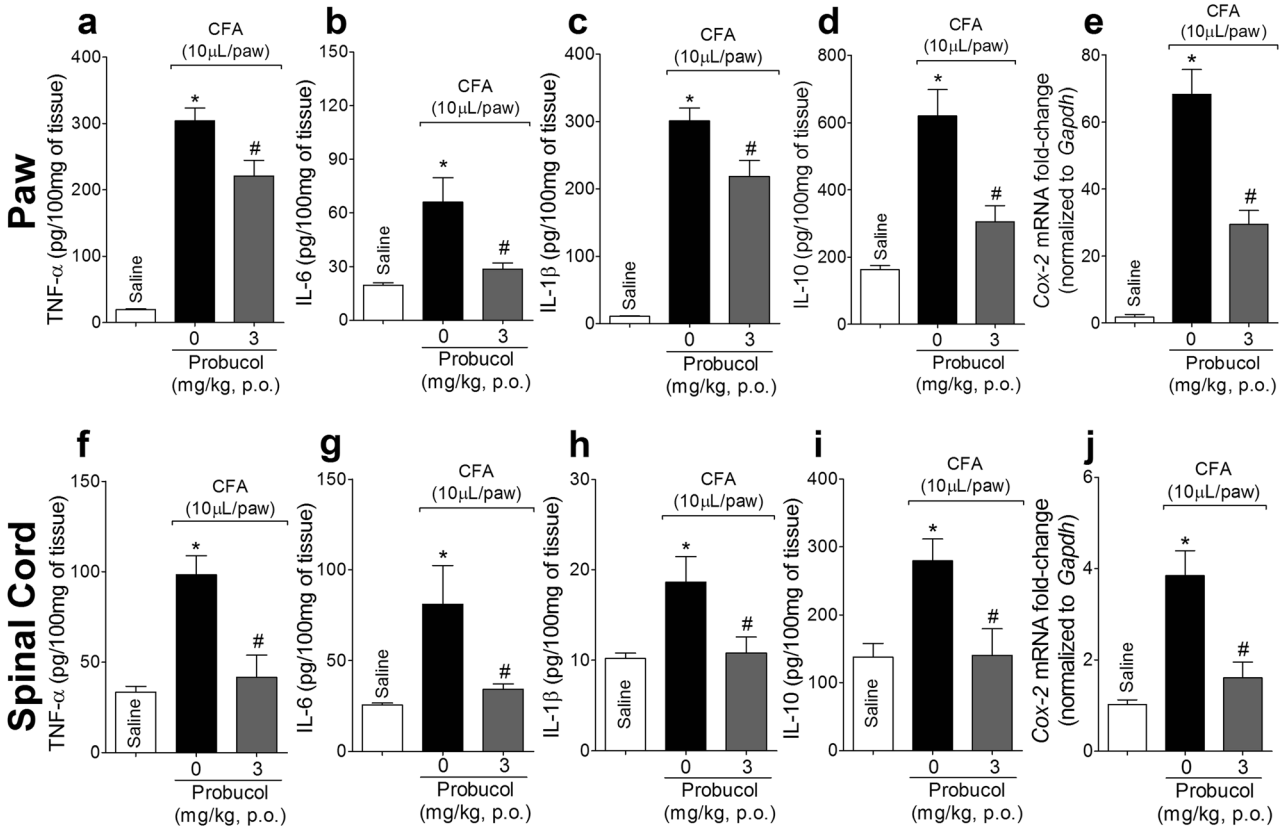

Fig. 5. Probucol inhibits CFA-induced cytokine secretion and *Cox-2* expression in paw tissue and spinal cord. Mice received probucol at 3 mg/kg (p.o.) daily 24 h after i.pl. injection of CFA (10 μL/paw). Paw skin and spinal cord tissue (L4–L6) were removed 3 days after CFA. TNF-α, IL-6, IL-1β, and IL-10 levels were measured in the paw skin (a-d) and in the spinal cord (f-i) by ELISA. *Cox*-2 mRNA expression was measured in the paw skin (e) and the spinal cord (j) by qPCR and normalized to *Gapdh* expression. The 0 mg/kg of probucol group stands for vehicle group. Results are expressed as mean ± SEM ($n = 6$ per group per experiment, representative of two separate experiments). One-way ANOVA followed by Tukey's post hoc. *$p < 0.05$ *vs.* saline group. #$p < 0.05$ *vs.* vehicle group.

behavior was evaluated over 30 min. Probucol inhibited CFA-induced paw flinches by 43% and time spent licking the paw by 42% (Fig. 2).

Probucol Inhibits CFA-Induced Astrocyte and Microglia Activation in the Spinal Cord

Mice were treated with probucol at 3 mg/kg p.o. or vehicle (Tween 80 5% in saline) daily starting 24 h after i.pl. administration of CFA (10 μL/paw). At 3 days after CFA i.pl. injection, mice were perfused with saline and 4% paraformaldehyde and the spinal cord (L4-L6) was dissected for immunostaining of GFAP and Iba-1, which are markers of astrocyte and microglia activation, respectively. Probucol inhibited CFA-induced glial activation as demonstrated by a reduction in both GFAP and Iba-1 fluorescence intensity in the dorsal horn of the spinal cord (Fig. 3).

Probucol Does Not Inhibit CFA-Induced ROS Production in Paw and Spinal Cord

Mice were treated with probucol at 3 mg/kg p.o. or vehicle (Tween 80 5% in saline) daily 24 h after i.pl. administration of CFA (10 μL/paw). Paw skin and spinal cord tissues were harvested 3 days after CFA i.pl. injection to evaluate the following parameters of oxidative stress: ABTS free radical scavenging ability, superoxide anion formation by NBT reduction, and lipid peroxidation by TBARS. CFA induced tissue oxidative stress in the paw and spinal cord observed as reduction of ABTS scavenging ability (22 and 40%, respectively) as well as superoxide anion formation (NBT reduction, 80 and 167%, respectively) and increase of lipid peroxidation (TBARS assay, 500 and 63%, respectively) compared to the saline group (Fig. 4a–f). Probucol at the dose of 3 mg/kg neither

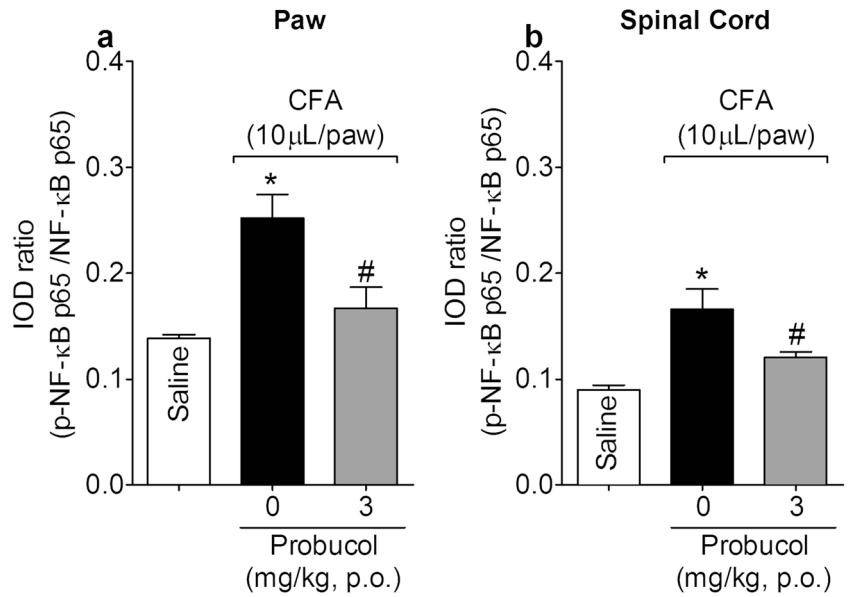

Fig. 6. Probucol inhibits CFA-induced NF-κB activation in paw tissue (**a**) and spinal cord (**b**). Mice received probucol at 3 mg/kg (p.o.) daily 24 h after i.pl. injection of CFA (10 μL/paw). Paw skin and spinal cord tissue (L4–L6) were removed 3 days after CFA. NF-κB activation was evaluated by ELISA. The 0 mg/kg of probucol group stands for vehicle group. Results are expressed as mean ± SEM ($n = 6$ per group per experiment, representative of two separate experiments). One-way ANOVA followed by Tukey's post hoc. *$p < 0.05$ *vs.* saline group. #$p < 0.05$ *vs.* vehicle group.

restored tissue antioxidant capacity nor reduced ROS formation ($p > 0.05$) (Fig. 4a–f).

Probucol Inhibits CFA-Induced Cytokine Production and Upregulation of Cyclooxygenase-2 (*Cox-2*) mRNA Expression in Paw and Spinal Cord

Mice were treated with probucol at 3 mg/kg p.o. or vehicle (Tween 80 5% in saline) daily starting 24 h after i.pl. administration of CFA (10 μL/paw). Paw skin and spinal cord tissues (L4-L6) were removed 3 days after CFA i.pl. injection. Probucol inhibited TNF-α (28% and 58%), IL-6 (56% and 58%), IL-1β (28% and 42%), and IL-10 (51% and 50%) production in the paw and spinal cord, respectively (Fig. 5a–d, f–i). To assess *Cox-2* expression, spinal cord tissues (L4-L6) were removed 3 days after CFA i.pl. injection and paw tissues were removed 27 h after CFA, *i.e.*, 3 h after a single post-treatment with probucol at 3 mg/kg. Different timepoints for spinal cord and paw tissues were based on time-response optimization experiments (data not shown). Probucol inhibited mRNA expression of *Cox-2* in both paw and spinal cord (Fig. 5e, j, respectively).

Probucol Inhibits CFA-Induced NF-κB Activation and Substance P Protein Expression

Mice were treated with probucol at 3 mg/kg p.o. or vehicle (Tween 80 5% in saline) daily starting 24 h after i.pl. administration of CFA (10 μL/paw). Paw skin and/or spinal cord tissue (L4-L6) were removed 3 days after CFA i.pl. injection. Probucol inhibited CFA-induced NF-κB activation in the paw tissue (36%) and spinal cord (29%) demonstrated by a reduction of CFA-induced increase of p-NF-κB p65/NF-κB p65 ratio (Fig. 6a, b, respectively). Moreover, treatment with probucol reduced both activation of NF-κB (*i.e.*, phosphorylation of NF-κB) and nuclear localization of phosphorylated NF-κB in the spinal cord tissue (L4-L6) 3 days after CFA i.pl (Fig. 7). Substance P expression in the spinal cord was also inhibited by daily treatment with probucol (Fig. 8).

Probucol Treatment Does Not Alter Parameters of Renal and Liver Function, Gastric Lesions

Mice were treated with probucol at 3 mg/kg p.o. or vehicle (Tween 80 5% in saline) for 7 days. Plasma levels of AST, ALT, creatinine, and urea were evaluated using commercial diagnostic kits as markers of hepatotoxicity and

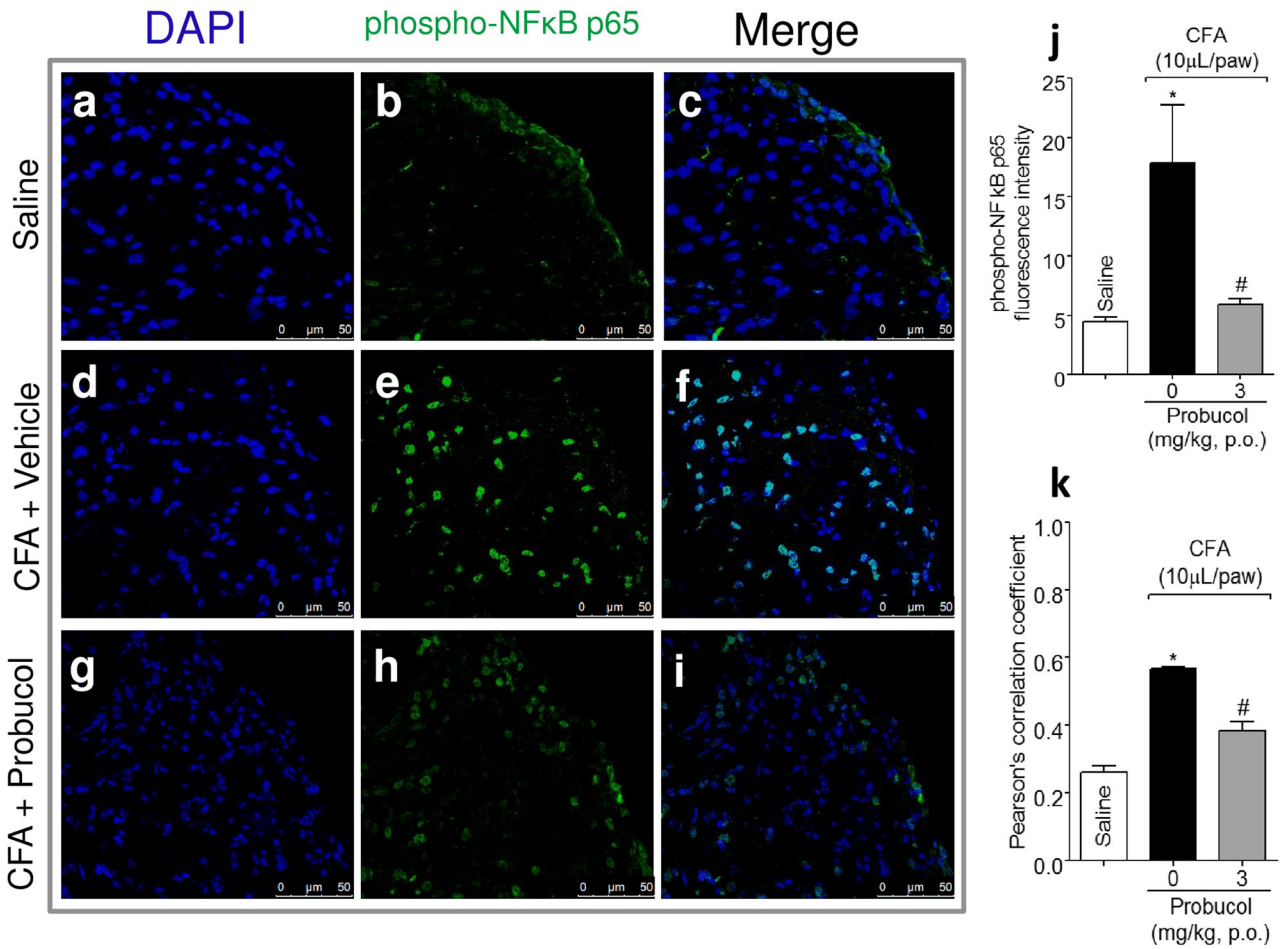

Fig. 7. Probucol inhibits CFA-induced NF-κB phosphorylation and nuclear localization of phosphorylated NF-κB in the spinal cord. Mice received probucol at 3 mg/kg (p.o.) daily 24 h after i.pl. injection of CFA (10 µL/paw). The spinal cord tissue (L4–L6) was removed 3 days after CFA. Phosphorylated NF-κB and nuclear localization of phosphorylated NF-κB in the spinal cord were evaluated by immunofluorescence. Representative images of DAPI and phospho-NF-κB p65 subunit stainings in the spinal cord for each experimental group are shown in a-i. Quantification of phospho-NF-κB p65 subunit fluorescent intesity is shown in j. Colocalization of DAPI and phospho-NF-κB p65 subunit stainings was expressed as Pearson's correlation coefficient (k). The 0 mg/kg of probucol group stands for vehicle group. Results are expressed as mean ± SEM ($n = 4$ per group per experiment, representative of two separate experiments). One-way ANOVA followed by Tukey's post hoc. *$p < 0.05$ *vs.* saline group. #$p < 0.05$ *vs.* vehicle group.

nephrotoxicity, respectively. Neutrophil recruitment in stomach was assessed by MPO assay as a marker of gastric lesion. Treatment with probucol did not alter any of the parameters evaluated when compared to the vehicle-treated group ($p > 0.05$). Acetaminophen, diclofenac, and indomethacin induced hepatotoxicity, nephrotoxicity, and gastric lesion, respectively ($p < 0.05$) (Fig. 9).

DISCUSSION

Up to 30% of adults suffer from chronic pain worldwide [5]. Persistent pain often becomes a limiting factor in most aspects of patients' lives, characterizing a relevant public health issue. Additionally, long-term treatment with currently used anti-inflammatory drugs presents a wide range of side effects also impairing patients' quality of life [6, 7]. In this context, we aimed to investigate the analgesic and anti-inflammatory potential of probucol.

In the present work, we showed that probucol inhibited CFA-induced thermal and mechanical hyperalgesia along with overt pain-like behavior. These results are in agreement with our previous findings, which investigated the peripheral effect of probucol in models of acute inflammatory pain after a single treatment 1 h before the stimulus [28, 29]. In this present work, however, we have evaluated both the

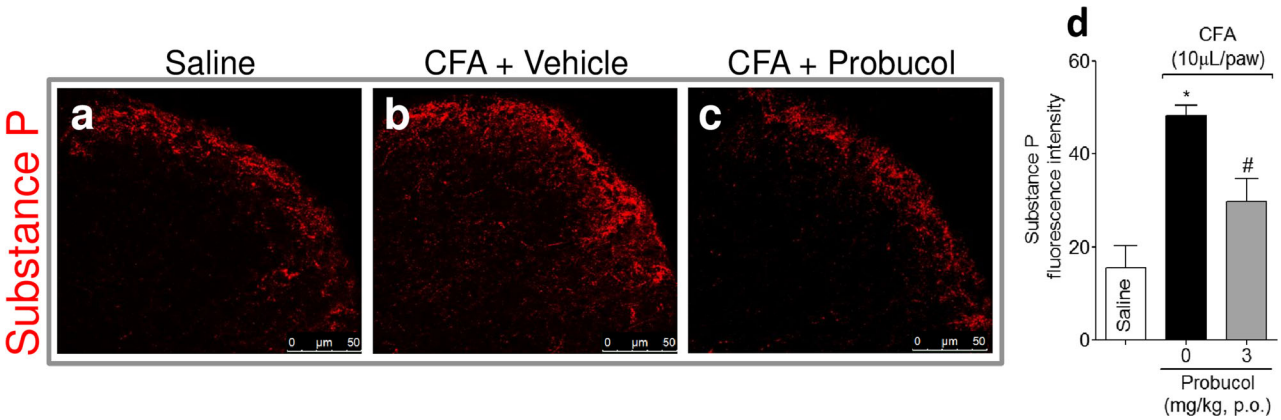

Fig. 8. Probucol inhibits CFA-induced production of substance P in the spinal cord. Mice received probucol at 3 mg/kg (p.o.) daily 24 h after i.pl. injection of CFA (10 µL/paw). The spinal cord tissue (L4–L6) was removed 3 days after CFA. Substance P levels in the spinal cord were evaluated by immunofluorescence. Representative images of Substance P staining in the spinal cord for each group are shown in a-c. Quantification of Substance P fluorescence intensity is shown in d. The 0 mg/kg of probucol group stands for vehicle group. Results are expressed as mean ± SEM ($n = 4$ per group per experiment, representative of two separate experiments). One-way ANOVA followed by Tukey's post hoc. *$p < 0.05$ *vs.* saline group. #$p < 0.05$ *vs.* vehicle group.

peripheral and spinal anti-inflammatory, antioxidant, and analgesic activity of probucol in a model of persistent pain. A low dose of probucol, given daily and starting 24 h after the inflammatory stimulus, inhibited thermal and mechanical hyperalgesia up to 7 days without causing any signs of gastric or impairing renal and liver functions.

In addition to its analgesic effect, probucol inhibited inflammation in the peripheral tissue (e.g., paw edema and MPO activity) and spinal cord (astrocyte and microglia activation) following CFA injection. In the peripheral inflammatory milieu, neutrophils secrete PGE_2 in response to IL-1β. In turn, PGE_2, a lipid mediator generated from arachidonic acid by COX-2, directly sensitizes nociceptors triggering hyperalgesia [41]. Therefore, inhibition of neutrophil influx, IL-1β production, and *Cox-2* mRNA expression in the paw tissue may contribute to the analgesic effects observed. Additionally, CFA components interact with a wide range of pattern recognition receptors (PRRs) eliciting an inflammatory response that persists for weeks. Previous studies have shown that CFA induces spinal activation provoking mechanical and thermal hyperalgesia in a NF-κB-dependent manner [15, 42]. At day 4 post-CFA, Zhu et al. (2014) observed mechanical and thermal hyperalgesia along with increased levels of TNF-α, IL-1β, and IL-6 in lumbar spinal cord. Additionally, mRNA expression and protein levels of Iba-1, a marker of microglia activation, were increased at the same time point [43]. *In vitro*, probucol inhibits LPS-induced activation of primary mouse microglia and BV2 microglia mouse cell line. Probucol inhibited LPS-induced NO release and production of IL-1β, IL-6, and PGE2 as well as inhibited NF-κB, MAPK, and AP- activation [44]. Thus, our *in vivo* data shows that probucol can inhibit glia cells activation, which is consistent with previous *in vitro* evidence [44]. TNF-α, IL-1β, and IL-6 were previously shown to be augmented in the spinal cord of rats as early as 4 h post-CFA [15, 45, 46]. Since no systemic levels of cytokines were detected earlier than 24 h after CFA and the blood-brain barrier permeability was not increased up to 5 days post-stimulus, it is likely that these pro-inflammatory cytokines are of central origin [47, 48]. In fact, microglia activation occurs as early as 4 h after CFA and maintained up to 14 days. In turn, astrocytes show a delayed activation, at day 4 [15]. Hartung et al. (2015) demonstrated a role of astrocyte-derived NF-κB in inhibiting expression of catechol-o-methyltransferase, an enzyme that inactivates catecholamines involved in nociception [42].

In agreement with previous studies, we have observed increased protein expression of Iba-1 and GFAP, *i.e.*, activation of microglia and astrocytes, in the lumbar spinal cord as well as increased levels of IL-1β, TNF-α, and IL-6 and *Cox-2* mRNA expression. These mediators were shown to play an important role in pain signaling by either direct sensitization of nociceptors or by triggering production of other hyperalgesic mediators [49–52]. Probucol-treated mice showed reduced peripheral and spinal cord levels of IL-1β, TNF-α, IL-6, and *Cox*-2 mRNA expression as well as reduced protein expression of GFAP and Iba-1. These findings suggest that inhibition of glial activation and cytokine production are involved in its analgesic mechanisms.

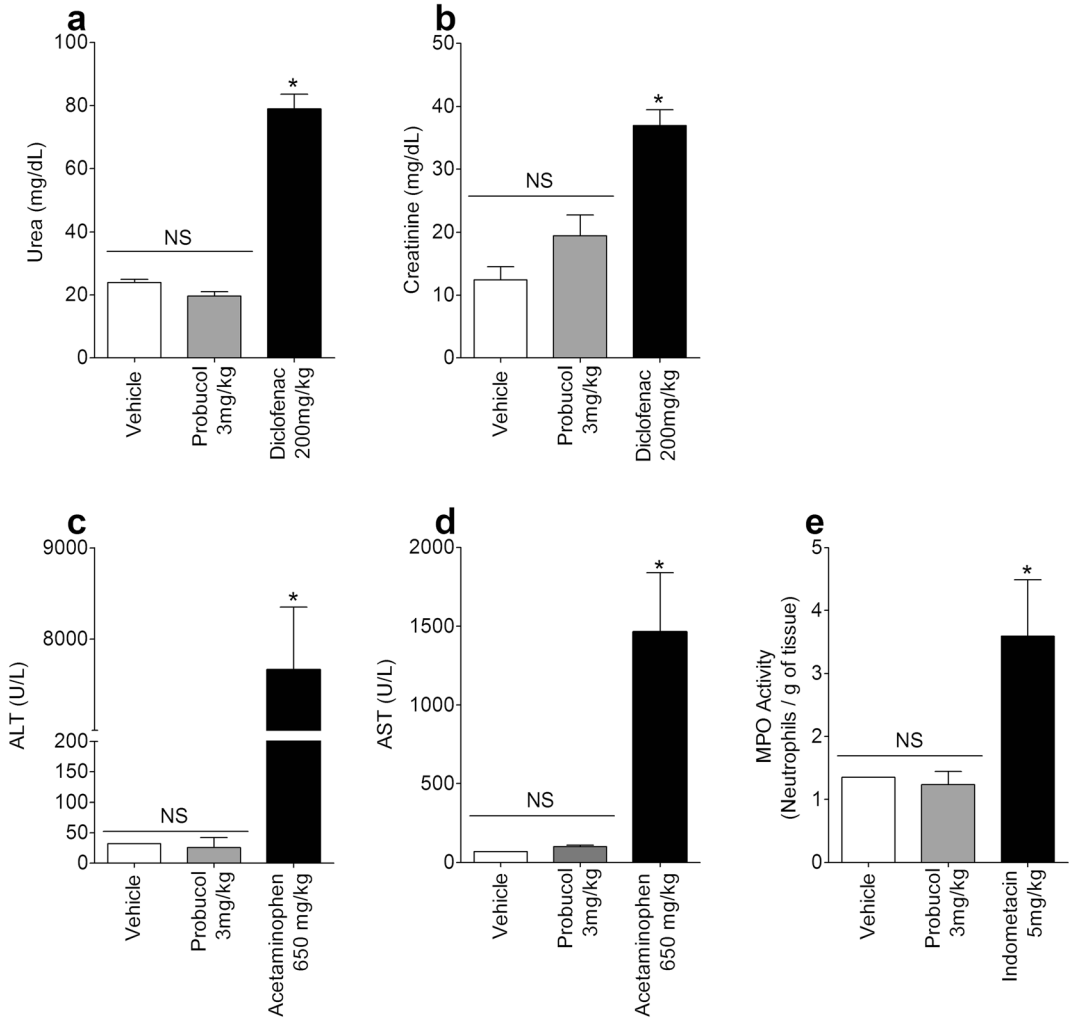

Fig. 9. Treatment with probucol did not affect renal or liver function or caused gastric lesions. Mice received probucol at 3 mg/kg (p.o.) daily for 7 days. Diclofenac (200 mg/kg, single dose, 24 h) was used as a positive control for nephrotoxicity. Acetaminophen (650 mg/kg, single dose, 10 h) was used as positive control for hepatotoxicity. Indomethacin (5 mg/kg, daily for 7 days) was used as a positive control for gastric lesion. Plasma was obtained to evaluate levels of urea, creatinine, ALT, and AST using commercial diagnostic kids. Stomach was removed to evaluate MPO activity. Results are expressed as mean ± SEM ($n = 6$ per group per experiment, representative of two separate experiments). One-way ANOVA followed by Tukey's post hoc. $^*p < 0.05$ *vs.* vehicle group.

In order to investigate putative anti-inflammatory mechanisms induced by probucol, we evaluated antioxidant ability as well as IL-10 production in both spinal cord and paw tissue. Despite previous evidence, we have not observed an antioxidant effect at the anti-inflammatory/analgesic dose chosen in this work [24, 53, 54]. Our contrasting result can be explained by the use of a remarkably lower dose administrated for a short period (3 days) in opposed to longer treatments with higher doses, up to 61 mg/kg/day in a model of inflammation following transient forebrain ischemia [24]. Therefore, our results suggest that probucol exerts anti-inflammatory and analgesic effects by employing mechanism other than its antioxidant properties. With regard to IL-10 levels, probucol inhibited its production in spinal cord as well as paw tissue suggesting that it acts on an upstream target, possibly NF-κB itself. In fact, probucol has been previously shown to reduce NF-κB nuclear translocation in endothelial cells [18, 23, 55].

The canonical NF-κB pathway is activated upon stimulation of PRRs, IL-1R, and TNFR1. Activated NF-κB translocates to nucleus triggering transcription

of adhesion molecules and pro-inflammatory mediators (*e.g.*, IL-1β, TNF-α, IL-6, and COX-2). Moreover, the NF-κB pathway displays a wide range of self-modulatory mechanisms. For instance, NF-κB promotes delayed transcription of anti-inflammatory mediators such as IL-10 [56, 57]. Indeed, by assessment of the p-NF-κB p65/total NF-κB p65 ratio in both paw and lumbar spinal cord, we have demonstrated the inhibitory effect of probucol on NF-κB activation. Probucol-treated animals also presented reduced nuclear localization of phosphorylated NF-κB in the L4-L6 segments of the spinal cord following CFA stimulus. To our knowledge, this is the first report to show probucol-mediated inhibition of spinal NF-κB activation and nuclear localization of phosphorylated NF-κB in an *in vivo* model of inflammatory pain.

Finally, to further assess the spinal mechanisms of probucol-induced analgesia, we evaluated the expression of substance P in the spinal dorsal horn. Substance P is a neuropeptide released by afferent sensory neurons in the dorsal horn of the spinal cord [58, 59]. Substance P is involved in pain signaling and subsequent mechanical hyperalgesia through activation of the neurokinin receptor 1 in nearby neurons, an effect counteracted by the Y1 receptor and its ligand neuropeptide Y [60]. Intraplantar injection of CFA has been shown to induce rapid mobilization and biosynthesis of substance P at 4 h post-stimulus, peaking at 4 days [14]. This effect was observed at the protein but not at the gene level, as the transcript level of substance P precursor, *Tac1*, remains unchanged over the course of 14 days [14]. Accordingly, we observed increased protein expression of substance P 3 days after CFA. This effect was inhibited by treatment with probucol. Thus, probucol-mediated inhibition of substance P may also underlie the analgesic activity of probucol, at the spinal level.

Taken together, our results strongly support that probucol alleviates persistent pain by inhibiting spinal and peripheral pro-hyperalgesic mediators in a NF-κB-dependent manner. Importantly, daily treatment with probucol did not affect renal or liver functions or caused gastric lesions, which are common side effects of NSAIDs [7]. Thus, our results broaden the clinical potential of probucol as a promising anti-inflammatory and analgesic drug. Nevertheless, it is also important to mention that probucol may affect the production of other hyperalgesic molecules since evidence support its inhibitory effect over AP-1 and MAPK [44].

ACKNOWLEDGMENTS

The authors would like to thank the technical support of Maria Rosana F. de Paula.

FUNDING

Conselho Nacional do Desenvolvimento Científico e Tecnológico (CNPq), Coordenação do Aperfeiçoamento de Pessoal de Nível Superior (CAPES), and Programa de Apoio a Grupos de Excelência (PRONEX) grant supported by SETI/Araucária Foundation, MCTI/CNPq, and Parana State Government (agreement 014/2017, protocol 46.843).

COMPLIANCE WITH ETHICAL STANDARDS

Conflict of Interest. The authors declare that they have no conflict of interest.

REFERENCES

1. Medzhitov, Ruslan. 2008. Origin and physiological roles of inflammation. *Nature* 454: 428–435. https://doi.org/10.1038/nature07201.
2. Ji, Ru-Rong, Zhen-Zhong Xu, and Yong-Jing Gao. 2014. Emerging targets in neuroinflammation-driven chronic pain. *Nature Reviews Drug Discovery* 13. NIH Public Access: 533–48. doi:https://doi.org/10.1038/nrd4334.
3. Maniadakis, N., and A. Gray. 2000. The economic burden of back pain in the UK. *Pain* 84: 95–103.
4. Moulin, Dwight E., Alexander J. Clark, Mark Speechley, and Patricia K. Morley-Forster. 2002. Chronic pain in Canada–prevalence, treatment, impact and the role of opioid analgesia. *Pain Research & Management* 7: 179–184.
5. Ji, Ru-rong, Alexander Chamessian, and Yu-qiu Zhang. 2016. Pain regulation by non-neuronal cells and inflammation. *Science* 354: 572–577.
6. Manson, Stephanie C., Ruth E. Brown, Annamaria Cerulli, and Carlos Fernandez Vidaurre. 2009. The cumulative burden of oral corticosteroid side effects and the economic implications of steroid use. *Respiratory Medicine* 103. Elsevier Ltd: 975–994. doi:https://doi.org/10.1016/j.rmed.2009.01.003.
7. Süleyman, Halis, Berna Demircan, and Yalçin Karagöz. 2007. Anti-inflammatory and side effects of cyclooxygenase inhibitors. *Pharmacological reports : PR* 59: 247–258.
8. Tapping, Richard I., and Peter S. Tobias. 2003. Mycobacterial lipoarabinomannan mediates physical interactions between TLR1 and TLR2 to induce signaling. *Journal of Endotoxin Research* 9: 264–268. https://doi.org/10.1179/096805103225001477.
9. Means, T.K., B.W. Jones, A.B. Schromm, B.A. Shurtleff, J.A. Smith, J. Keane, D.T. Golenbock, S.N. Vogel, and M.J. Fenton. 2001. Differential effects of a Toll-like receptor antagonist on *Mycobacterium tuberculosis*-induced macrophage responses. *Journal*

of immunology (Baltimore, Md. : 1950) 166. American Association of Immunologists: 4074–82. doi:https://doi.org/10.4049/JIMMUNOL.166.6.4074.

10. Yadav, Mahesh, and Jeffrey S Schorey. 2006. The beta-glucan receptor dectin-1 functions together with TLR2 to mediate macrophage activation by mycobacteria. *Blood* 108. American Society of Hematology: 3168–75. doi:https://doi.org/10.1182/blood-2006-05-024406.
11. Ferwerda, Gerben, Stephen E. Girardin, Bart-Jan Kullberg, Lionel Le Bourhis, Dirk J. de Jong, Dennis M. L. Langenberg, Reinout van Crevel, et al. 2005. NOD2 and toll-like receptors are nonredundant recognition systems of Mycobacterium tuberculosis. *PLoS Pathogens* 1. **Public Library of Science: e34**. doi:https://doi.org/10.1371/journal.ppat.0010034.
12. Underhill, D.M., A. Ozinsky, K.D. Smith, and A. Aderem. 1999. Toll-like receptor-2 mediates mycobacteria-induced proinflammatory signaling in macrophages. *Proceedings of the National Academy of Sciences of the United States of America* 96. National Academy of Sciences: 14459–63.
13. Kleinnijenhuis, Johanneke, Leo A. B. Joosten, Frank L. van de Veerdonk, Nigel Savage, Reinout van Crevel, Bart Jan Kullberg, Andre van der Ven, et al. 2009. Transcriptional and inflammasome-mediated pathways for the induction of IL-1β production by *Mycobacterium tuberculosis*. *European Journal of Immunology* 39. WILEY-VCH Verlag: 1914–1922. doi:https://doi.org/10.1002/eji.200839115.
14. Maduka, U.P., M.V. Hamity, R.Y. Walder, S.R. White, Y. Li, and D.L. Hammond. 2016. Changes in the disposition of substance P in the rostral ventromedial medulla after inflammatory injury in the rat. *Neuroscience* 317: 1–11. https://doi.org/10.1016/j.neuroscience.2015.12.054.
15. Raghavendra, Vasudeva, Flobert Y. Tanga, and Joyce A. Deleo. 2004. Complete Freunds adjuvant-induced peripheral inflammation evokes glial activation and proinflammatory cytokine expression in the CNS. *European Journal of Neuroscience* 20: 467–473. https://doi.org/10.1111/j.1460-9568.2004.03514.x.
16. Yamamoto, A., H. Hara, S. Takaichi, J. Wakasugi, M. Tomikawa, S.G. Baker, B.I. Joffe, et al. 1988. Effect of probucol on macrophages, leading to regression of xanthomas and atheromatous vascular lesions. *The American journal of cardiology* 62. Elsevier: 31B–36B. doi:https://doi.org/10.1016/S0002-9149(88)80048-1.
17. Bridges, A.B., N.A. Scott, and J.J.F. Belch. 1991. Probucol, a superoxide free radical scavenger in vitro. *Atherosclerosis* 89: 263–265. https://doi.org/10.1016/0021-9150(91)90068-E.
18. Aoki, M., T. Nata, R. Morishita, H. Matsushita, H. Nakagami, K. Yamamoto, K. Yamazaki, M. Nakabayashi, T. Ogihara, and Y. Kaneda. 2001. Endothelial apoptosis induced by oxidative stress through activation of NF-κB: Antiapoptotic effect of antioxidant agents on endothelial cells. *Hypertension* 38: 48–55. https://doi.org/10.1161/01.HYP.38.1.48.
19. Akeson, Ann L., Connie W. Woods, Laura B. Mosher, Craig E. Thomas, and Richard L. Jackson. 1991. Inhibition of IL-1b expression in THP-1 cells by probucol and tocopherol. *Atherosclerosis* 86: 261–270. https://doi.org/10.1016/0021-9150(91)90222-O.
20. Kaneko, M., J. Hayashi, I. Saito, and N. Miyasaka. 1996. Probucol downregulates E-selectin expression on cultured human vascular endothelial cells. *Arteriosclerosis, Thrombosis, and Vascular Biology* 16: 1047–1051. https://doi.org/10.1161/01.ATV.16.8.1047.
21. Liu, Ge-Xiu, Da-Ming Ou, Jun-Hua Liu, Hong-Lin Huang, and Duan-Fang Liao. 2000. Probucol inhibits lipid peroxidation of macrophage and affects its secretory properties. *Acta Pharmacologica Sinica* 21: 637–640.
22. Zapolska-Downar, D., A. Zapolski-Downar, M. Markiewski, A. Ciechanowicz, M. Kaczmarczyk, and M. Naruszewicz. 2000. Selective inhibition by alpha-tocopherol of vascular cell adhesion molecule-1 expression in human vascular endothelial cells. *Biochemical and Biophysical Research Communications* 155: 609–615. https://doi.org/10.1006/bbrc.2000.3197.
23. Zhang, M., J. Wang, J.H. Liu, S.J. Chen, B. Zhen, C.H. Wang, H. He, and C.X. Jiang. 2013. Effects of probucol on angiotensin II-induced BMP-2 expression in human umbilical vein endothelial cells. *Molecular Medicine Reports* 7: 177–182. https://doi.org/10.3892/mmr.2012.1145.
24. Al-Majed, Abdulhakeem a. 2011. Probucol attenuates oxidative stress, energy starvation, and nitric acid production following transient forebrain ischemia in the rat hippocampus. *Oxidative Medicine and Cellular Longevity* 2011: 1–8. https://doi.org/10.1155/2011/471590.
25. Li, S., J. Liang, M. Niimi, A. Bilal Waqar, D. Kang, T. Koike, Y. Wang, M. Shiomi, and J. Fan. 2014. Probucol suppresses macrophage infiltration and MMP expression in atherosclerotic plaques of WHHL rabbits. *Journal of Atherosclerosis and Thrombosis* 21: 648–658. https://doi.org/10.5551/jat.21600.
26. Li, Tingting, Wenqiang Chen, Fengshuang An, Hongbo Tian, Jianning Zhang, Jie Peng, Yun Zhang, and Yuan Guo. 2011. Probucol attenuates inflammation and increases stability of vulnerable atherosclerotic plaques in rabbits. *The Tohoku Journal of Experimental Medicine* 225: 23–34. https://doi.org/10.1620/tjem.225.23.
27. Zhang, Xia, Zhongzhuan Li, Dongfang Liu, Xin Xu, Wei Shen, and Zhechuan Mei. 2009. Effects of probucol on hepatic tumor necrosis factor-alpha, interleukin-6 and adiponectin receptor-2 expression in diabetic rats. *Journal of Gastroenterology and Hepatology* 24: 1058–1063. https://doi.org/10.1111/j.1440-1746.2008.05719.x.
28. Zucoloto, Amanda Z., Marília F. Manchope, Larrisa Staurengo-Ferrari, José C. Alves-Filho, Thiago M. Cunha, Maísa M. Antunes, Gustavo B. Menezes, Fernando Q. Cunha, Rubia Casagrande, and Waldiceu A. Verri. 2017. Probucol attenuates overt pain-like behavior and carrageenan-induced inflammatory hyperalgesia and leukocyte recruitment by inhibiting NF-κB activation and cytokine production without antioxidant effects. *Inflammation Research* 66: 591–602. https://doi.org/10.1007/s00011-017-1040-8.
29. Zucoloto, Amanda Z., Marília F. Manchope, Larissa Staurengo-Ferrari, Felipe A. Pinho-Ribeiro, Ana C. Zarpelon, André L.L. Saraiva, Nerry Tatiana Cecílio, José C. Alves-Filho, Thiago M. Cunha, Gustavo B. Menezes, Fernando Q. Cunha, Rubia Casagrande, and Waldiceu A. Verri Jr. 2017. Probucol attenuates lipopolysaccharide-induced leukocyte recruitment and inflammatory hyperalgesia: Effect on NF-κB activation and cytokine production. *European Journal of Pharmacology* 809: 52–63. https://doi.org/10.1016/j.ejphar.2017.05.016.
30. Mizokami, Sandra S., Nilton S. Arakawa, Sergio R. Ambrosio, Ana C. Zarpelon, Rubia Casagrande, Thiago M. Cunha, Sergio H. Ferreira, Fernando Q. Cunha, and Waldiceu A. Verri. 2012. Kaurenoic acid from Sphagneticola trilobata inhibits inflammatory pain: Effect on cytokine production and activation of the NO-cyclic GMP-protein kinase G-ATP-sensitive potassium channel signaling pathway. *Journal of Natural Products* 75: 896–904. https://doi.org/10.1021/np200989t.
31. Navarro, Suelen A., Karla G.G. Serafim, Sandra S. Mizokami, Miriam S.N. Hohmann, Rubia Casagrande, and Waldiceu A.Jr. Verri. 2013. Analgesic activity of piracetam: Effect on cytokine production and oxidative stress. *Pharmacology Biochemistry and Behavior* 105: 183–192. https://doi.org/10.1016/j.pbb.2013.02.018.

32. Cunha, T.M., W.A. Jr Verri, G.G. Vivancos, I.F. Moreira, S. Reis, C.A. Parada, Fernando Q. Cunha, and S.H. Fereira. 2004. An electronic pressure-meter nociception paw test for rats. *Brazilian Journal of Medical and Biological Research* 37: 401–407. https://doi.org/10.1590/S0100-879X2004000300018.
33. Kuraishi, Y., Y. Harada, S. Aratani, M. Satoh, and H. Takagi. 1983. Separate involvement of the spinal noradrenergic and serotonergic systems in morphine analgesia: The differences in mechanical and thermal algesic tests. *Brain Research* 273: 245–252. https://doi.org/10.1016/0006-8993(83)90849-1.
34. Bradley, P., and D. Christensen. 2016. Cellular and extracellular Myeloperoxidade in pyogenic inflammation. *Blood* 60: 618–623.
35. Rossaneis, Ana C., Daniela T. Longhi-Balbinot, Mariana M. Bertozzi, Victor Fattori, Carina Z. Segato-Vendrameto, Stephanie Badaro-Garcia, Tiago H. Zaninelli, Larissa Staurengo-Ferrari, Sergio M. Borghi, Thacyana T. Carvalho, Allan J. C. Bussmann, Florêncio S. Gouveia Jr, Luiz G. F. Lopes, Rubia Casagrande, Waldiceu A. Verri Jr 2019. [Ru(bpy)2(NO)SO3](PF6), a nitric oxide donating ruthenium complex, reduces gout arthritis in mice. *Frontiers in Pharmacology* 10. **Frontiers**: 229. doi:https://doi.org/10.3389/FPHAR.2019.00229.
36. Zarpelon, Ana C., Francielle C. Rodrigues, Alexandre H. Lopes, Guilherme R. Souza, Thacyana T. Carvalho, Larissa G. Pinto, Xu Damo, et al. 2016. Spinal cord oligodendrocyte-derived alarmin IL-33 mediates neuropathic pain. *FASEB Journal* 30: 54–65. https://doi.org/10.1096/fj.14-267146.
37. Hohmann, Miriam S.N., Renato D.R. Cardoso, Felipe A. Pinho-Ribeiro, Jefferson Crespigio, Thiago M. Cunha, José C. Alves-Filho, Rosiane V. da Silva, et al. 2013. 5-Lipoxygenase deficiency reduces acetaminophen-induced hepatotoxicity and lethality. *BioMed research international* 2013. Hindawi Publishing Corporation: 627046. doi:https://doi.org/10.1155/2013/627046.
38. Curtis, R. Mason, and Marco L.A. Sivilotti. 2015. A descriptive analysis of aspartate and alanine aminotransferase rise and fall following acetaminophen overdose. *Clinical Toxicology* 53: 849–855. https://doi.org/10.3109/15563650.2015.1077968.
39. Fracasso, M.E., L. Cuzzolin, P. Del Soldato, R. Leone, G.P. Velo, and G. Benoni. 1987. Multisystem toxicity of indomethacin: Effects on kidney, liver and intestine in the rat. *Agents and Actions* 22: 310–313.
40. Syed, Nawazish-I-Husain, Farnaz Zehra, Amir Ali-Rizvi Syed, Sabiha Karim, and Farrakh Zia Khan. 2012. Comparing the effects of salts of diclofenac and alminoprofen with aspirin on serum electrolytes, creatinine and urea levels in rabbits. *Pakistan Journal of Pharmaceutical Sciences* 25: 777–782.
41. Cunha, Thiago M., W.A. Jr Verri, Ieda R. Schivo, Marcelo H. Napimoga, Carlos a Parada, Stephen Poole, Mauro M. Teixeira, Sergio H. Ferreira, and Fernando Q. Cunha. 2008. Crucial role of neutrophils in the development of mechanical inflammatory hypernociception. *Journal of Leukocyte Biology* 83: 824–832. https://doi.org/10.1189/jlb.0907654.
42. Hartung, Jane E., Olivia Eskew, Terrence Wong, Inna E. Tchivileva, Folabomi A. Oladosu, Sandra C. O'Buckley, and Andrea G. Nackley. 2015. Nuclear factor-kappa B regulates pain and COMT expression in a rodent model of inflammation. *Brain, Behavior, and Immunity* 50: 196–202. https://doi.org/10.1016/j.bbi.2015.07.014.
43. Zhu, Ming Di, Lin Xia Zhao, Xiao Tian Wang, Yong Jing Gao, and Zhi Jun Zhang. 2014. Ligustilide inhibits microglia-mediated proinflammatory cytokines production and inflammatory pain. *Brain Research Bulletin* 109. **Elsevier Inc.: 54–60**. doi:https://doi.org/10.1016/j.brainresbull.2014.10.002.
44. Jung, Yeon Suk, Jung Hwa Park, Hyunha Kim, So Young Kim, Ji Young Hwang, Ki Whan Hong, Sun Sik Bae, Byung Tae Choi, Sae-Won Lee, and Hwa Kyoung Shin. 2016. Probucol inhibits LPS-induced microglia activation and ameliorates brain ischemic injury in normal and hyperlipidemic mice. *Acta Pharmacologica Sinica* 37. Nature Publishing Group: 1031–44. doi:https://doi.org/10.1038/aps.2016.51.
45. Xu, Fei, Youhan Li, Shuo Li, Yunqing Ma, Ning Zhao, Yong Liu, Niansong Qian, Hong Zho, and Yu Li. 2014. Complete Freund's adjuvant-induced acute inflammatory pain could be attenuated by triptolide via inhibiting spinal glia activation in rats. *The Journal of Surgical Research* 188. Elsevier: 174–82. doi:https://doi.org/10.1016/j.jss.2013.11.1087.
46. Sun, Shukai, Yue Yin, Xin Yin, Fale Cao, Daoshu Luo, Ting Zhang, Yunqing Li, and Longxing Ni. 2012. Anti-nociceptive effects of Tanshinone IIA (TIIA) in a rat model of complete Freund's adjuvant (CFA)-induced inflammatory pain. *Brain Research Bulletin* 88: 581–588. https://doi.org/10.1016/j.brainresbull.2012.06.002.
47. Reiber, H., A.J. Suckling, and M.G. Rumsby. 1984. The effect of Freund's adjuvants on blood-cerebrospinal fluid barrier permeability. *Journal of the Neurological Sciences* 63: 55–61.
48. Samad, T.A., K.A. Moore, A. Sapirstein, S. Billet, A. Allchorne, S. Poole, J.V. Bonventre, and C.J. Woolf. 2001. Interleukin-1beta-mediated induction of Cox-2 in the CNS contributes to inflammatory pain hypersensitivity. *Nature* 410: 471–475. https://doi.org/10.1038/35068566.
49. Binshtok, A.M., H. Wang, and K. Zimmermann. 2008. Nociceptors are interleukin-1ßSensors. *The Journal of Neuroscience* 28: 14062–14073. https://doi.org/10.1523/JNEUROSCI.3795-08.2008.Nociceptors.
50. Cunha, T.M., W.A. Jr Verri, J.S. Silva, S. Poole, F.Q. Cunha, and S.H. Ferreira. 2005. A cascade of cytokines mediates mechanical inflammatory hypernociception in mice. *Proceedings of the National Academy of Sciences of the United States of America* 102: 1755–1760. https://doi.org/10.1073/pnas.0409225102.
51. Jin, X., W. Robert, and I.V. Gereau. 2006. Acute p38-mediated modulation of Tetrodotoxin-resistant sodium channels in mouse sensory neurons by tumor necrosis factor-a. *Journal of Neuroscience* 26: 246–255. https://doi.org/10.1523/JNEUROSCI.3858-05.2006.
52. Vazquez, Enrique, Jan Kahlenbach, Gisela Segond von Banchet, Christian König, Hans-Georg Schaible, and Andrea Ebersberger. 2012. Spinal interleukin-6 is an amplifier of arthritic pain in the rat. *Arthritis and Rheumatism* 64: 2233–2242. https://doi.org/10.1002/art.34384.
53. Colle, Dirleise, Danúbia Bonfanti Santos, Eduardo Luiz Gasnhar Moreira, Juliana Montagna Hartwig, Alessandra Antunes dos Santos, Luciana Teixeira Zimmermann, Mariana Appel Hort, and Marcelo Farina. 2013. Probucol increases striatal glutathione peroxidase activity and protects against 3-nitropropionic acid-induced pro-oxidative damage in rats. *PLoS One* 8: e67658. https://doi.org/10.1371/journal.pone.0067658.
54. Siveski-Iliskovic, N., N. Kaul, and P.K. Singal. 1994. Probucol promotes endogenous antioxidants and provides protection against adriamycin-induced cardiomyopathy in rats. *Circulation* 89: 2829–2835. https://doi.org/10.1161/01.CIR.89.6.2829.
55. Chang, Weng Cheng, Chia Hsin Chen, Ming Fen Lee, Ted Chang, and Ya Mei Yu. 2010. Chlorogenic acid attenuates adhesion molecules upregulation in IL-1b-treated endothelial cells. *European Journal of Nutrition* 49: 267–275. https://doi.org/10.1007/s00394-009-0083-1.
56. Ghosh, Sankar, and Matthew S. Hayden. 2008. New regulators of NF-kB in inflammation. *Nature Reviews Immunology* 8: 837–848. https://doi.org/10.1038/nri2423.
57. Cao, S., X. Zhang, Justin P. Edwards, and David M. Mosser. 2006. NF-kB1 (p50) homodimers differentially regulate pro- and anti-

inflammatory cytokines in macrophages. *Journal of Biological Chemistry* 281: 26041–26050. https://doi.org/10.1074/jbc.M602222200.

58. McLeod, A.L., J.E. Krause, A.C. Cuello, and A. Ribeiro-da-Silva. 1998. Preferential synaptic relationships between substance P-immunoreactive boutons and neurokinin 1 receptor sites in the rat spinal cord. *Proceedings of the National Academy of Sciences* 95: 15775–15780. https://doi.org/10.1073/pnas.95.26.15775.
59. Thomson, Lisa M., Gregory W. Terman, Jinsong Zeng, Janet Lowe, Charles Chavkin, Sam M. Hermes, Deborah M. Hegarty, and Sue A. Aicher. 2008. Decreased substance P and NK1 receptor immunoreactivity and function in the spinal cord dorsal horn of morphine-treated neonatal rats. *The Journal of Pain* 9: 11–19. https://doi.org/10.1016/j.jpain.2007.07.008.
60. Taylor, B.K., W. Fu, K.E. Kuphal, C.-O. Stiller, M.K. Winter, W. Chen, G.F. Corder, J.H. Urban, K.E. McCarson, and J.C. Marvizon. 2014. Inflammation enhances Y1 receptor signaling, neuropeptide Y-mediated inhibition of hyperalgesia, and substance P release from primary afferent neurons. *Neuroscience* 256: 178–194. https://doi.org/10.1016/j.neuroscience.2013.10.054.